

Supporting information

**An efficient localized catalytic hairpin assembly-based DNA
nanomachine for miRNA-21 imaging in living cells**

Juan Wu, Yonghui Tian, Lu He, Jing Zhang, Zhijun Huang, Zewei Luo*, Yixiang Duan*

Research Center of Analytical Instrumentation, Key Laboratory of Synthetic and Natural Functional Molecule Chemistry of Ministry of Education, College of Chemistry & Materials Science, Northwest University, Xi'an, 710069, Shaanxi, P.R.China;

* Corresponding Author: Zewei Luo, Yixiang Duan

Email: zwluo@nwu.edu.cn; yduan@nwu.edu.cn

Tables:

Table S1. Sequences details of synthesized oligonucleotides.

oligonucleotides.	Sequences (5'-3')
miRNA-21	UAGCUUAUCAGACUGAUGUUGA
H1	GACGACTAATAAGATTAATCCTGTCCTCAACATCAGTCTGA TAAGCTAATGTTGATTGGATGCTCTAGCTTATCAGACTG- TAMRA
H2	TGTCCTAATTAGAATAATCTCGAGTTCTAAGCTAGAGCATC CAATCAACATTAGCTTATCAGACTGATGTTGATTGGATGCT C
Stator strand	FAM- AACAGGATTAATCTTATTAGTCGTCCTCGAGATTATTCTAAT TAGGACAGCAGTTGAGGTAATAGTCACG
Free-H2	TTTTTTTTTTTTTTTTTTTTTTTTTTTTTTTCTAAGCTAGAGCATCCAA TCAACATTAGCTTATCAGACTGATGTTGATTGGATGCTC
One-base mismatched miRNA-21 1	TAGCTTATCAGACTGATGTAGA
One-base mismatched miRNA-21 2	TAGCTTATCAGACTGAAGTTGA
Two-base mismatched miRNA-21 1	TAGCTTATCAGAATGATGTAGA
Two-base mismatched miRNA-21 2	TAGCTAATCAGACTGATGATGA
Two-base mismatched miRNA-21 3	TTGCTTATCAGACTGAAGTTGA
Aptamer AS1411	GGTGGTGGTGGTGTGGTGGTGGTGGTTTTTCGTACTATTAC CTCAACTGC

The purple parts in H1, H2 represented binding region with the same color in stator stands, respectively. The green part represented the stem of hairpin structures. The red part of miRNA-21 analogues represents mismatch sites. The target miRNA-21 and analogues were replaced by corresponding DNA sequences in vitro experiments due to the low-cost and easy synthesis of DNA. And more importantly, the miRNA and the corresponding DNA showed same base-pairing recognitions which will produce similar response from the LCHA nanomachine.

Table S2. Sequences details of primers used in qRT-PCR analysis

miRNA-21	Stem-loop RT primer (5' to 3')	GTCGTATCCAGTGCAGGGTCCGAGGTATTTCGCACTG GATACGACTCAACA
	Forward primer (5' to 3')	GCGCTAGCTTATCAGACTGA
	Reverse primer (5' to 3')	GTGCAGGGTCCGAGGT
U-6	RT primer (5' to 3')	TTCACGAATTTGCGTGTCATC
	Forward primer (5' to 3')	CGCTTCGGCAGCACATATAC
	Reverse primer (5' to 3')	TTCACGAATTTGCGTGTCATC

Figures:

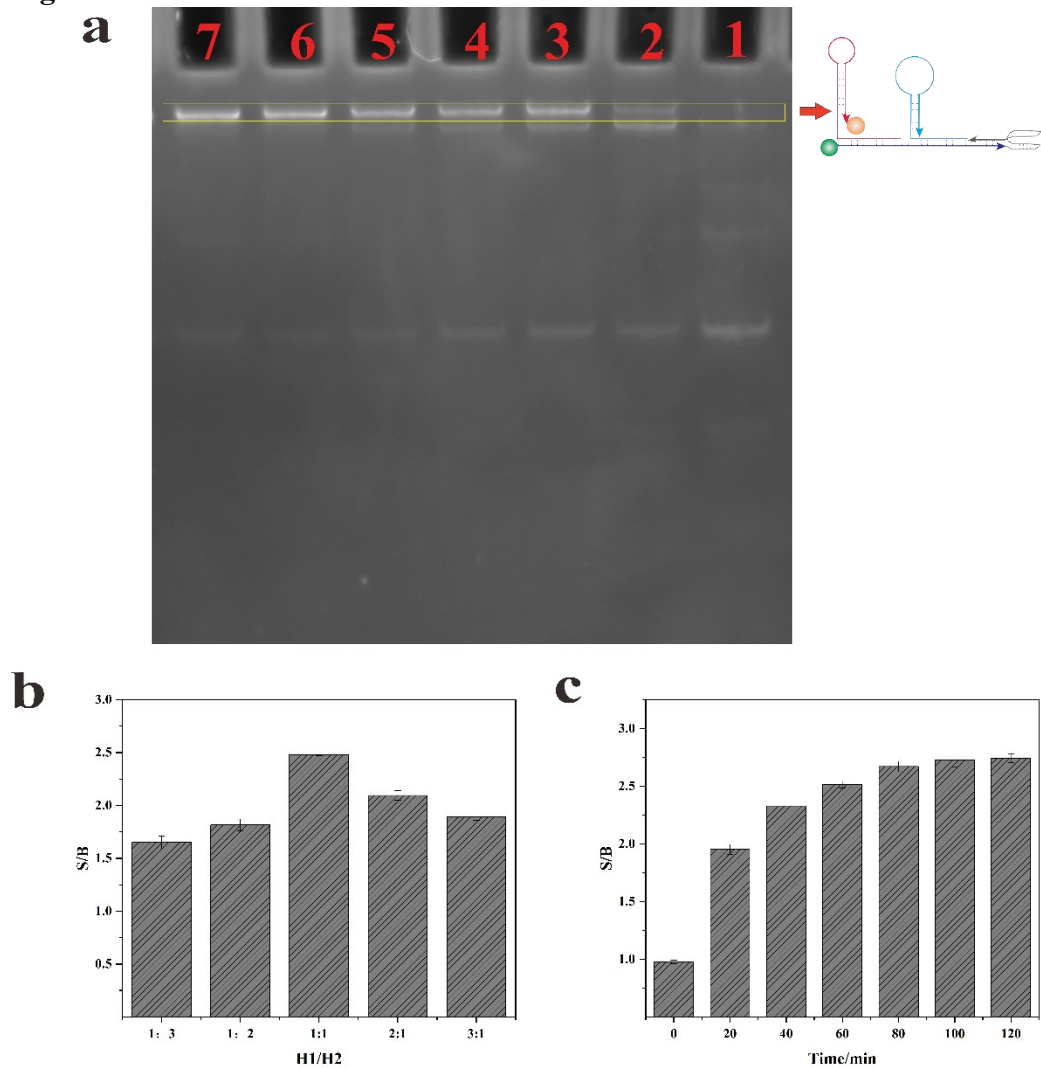


Fig. S1 Optimization of experimental conditions, including (a) the assembly time of LCHA nanomachine (from 1 to 7: 0 min, 15min, 30 min, 45 min, 60 min, 75min, 90min), (b) the concentration ratio of hairpin probes (H1 to H2, the concentration of H2 of 50 nM was fixed), and (c) the reaction time of LCHA reaction. In (b) and (c), S/B was the ratio of signal and background, where signal and background represent the F_{FAM}/F_{TAMRA} of LCHA nanomachine in the presence and absence of the target miRNA-21 of 20 nM, respectively.

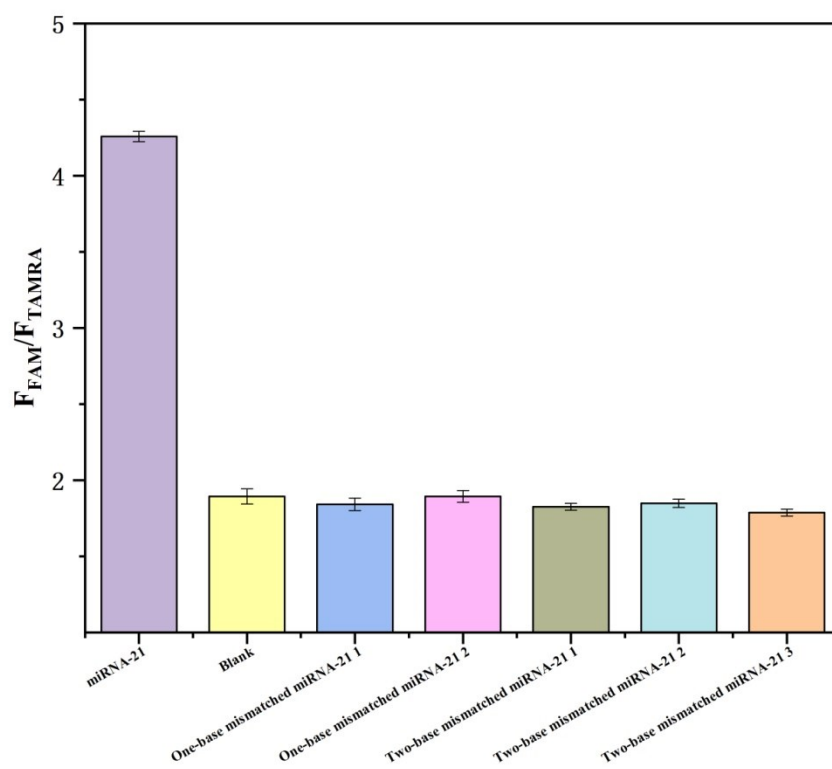


Fig. S2 Specificity evaluation of LCHA nanomachine. Comparison of the fluorescence intensity ratio in the presence of equal concentration of miRNA-21, one-base mismatched miRNA-21 1, one-base mismatched miRNA-21 2, two-base mismatched miRNA-21 1, two-base mismatched miRNA-21 2, two-base mismatched miRNA-21 3, respectively. In blank group, equal volume of PBS buffer displaced the miRNA-21.

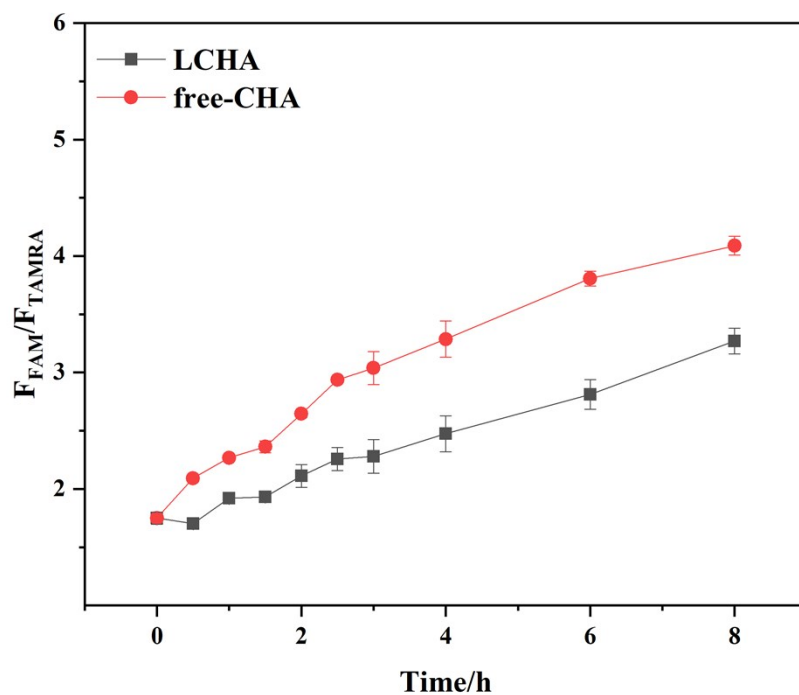


Fig.

S3 The stability analysis of LCHA nanomachine and free-CHA nanomachine in 10% FBS. The nanomachine with concentration of 50 nM was incubated at 37°C.

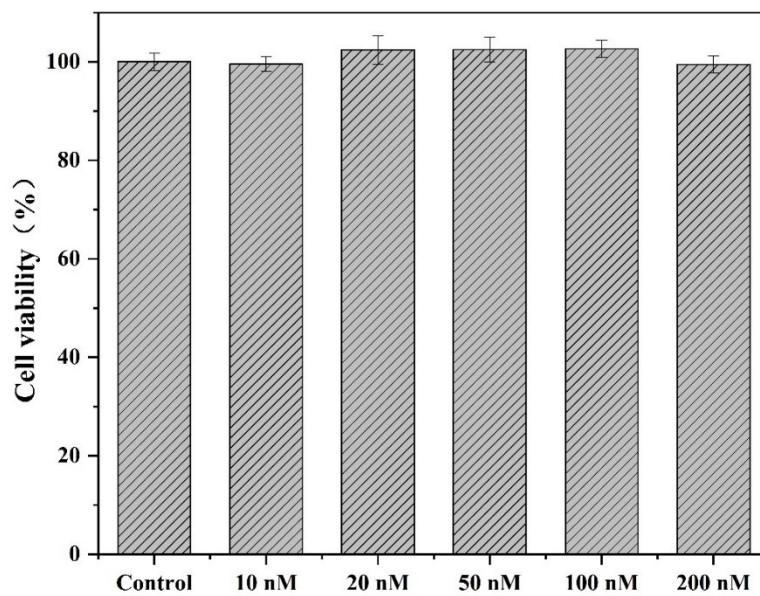


Fig. S4 Cytotoxicity of the LCHA nanomachine incubated with MCF-7 cells at different concentrations of probes (from left to right: 10 nM, 20 nM, 50 nM, 100 nM and 200 nM). In control group, equal volume of PBS buffer displaced the LCHA nanomachine.

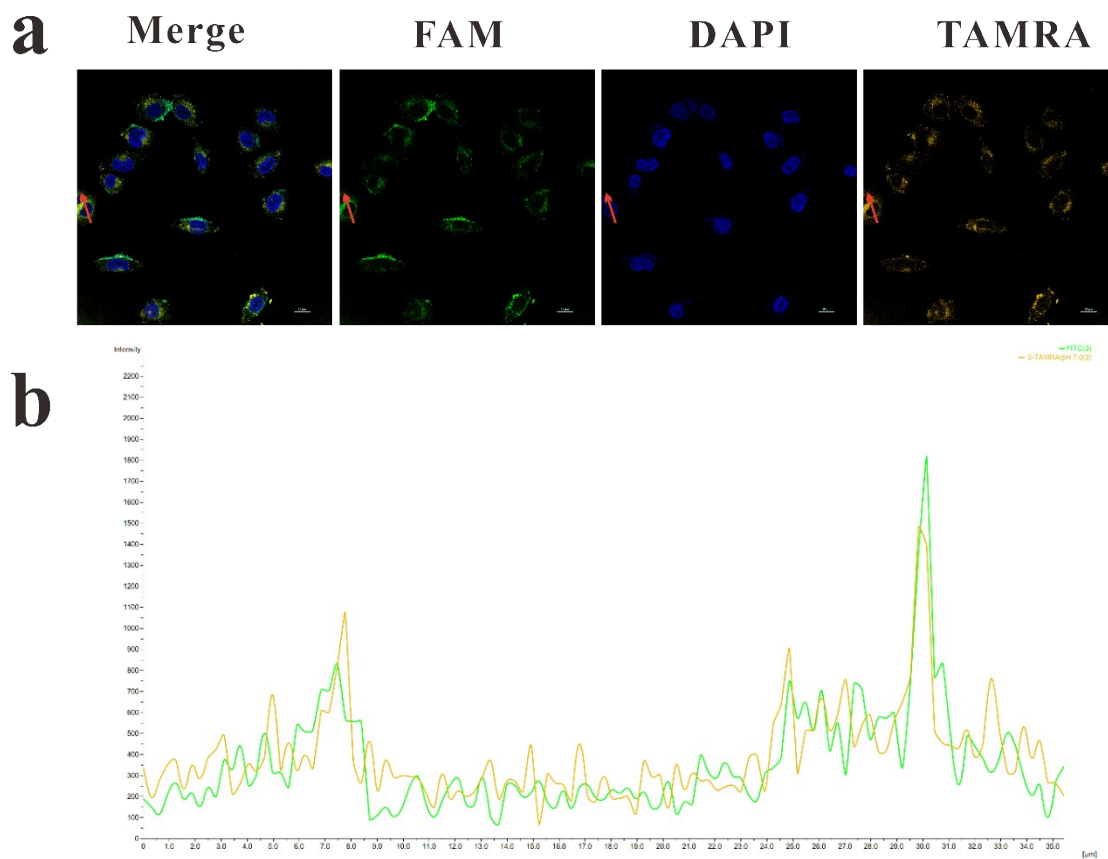


Fig. S5 Fluorescence co-localization of LCHA nanomachine in living cancer cells. (a) Confocal images of MCF-7 cells after incubating with LCHA nanomachine for 4 h followed by staining with DAPI for 15 min. Scale bar = 20 μm . (b) FAM (green) and TAMRA (orange) fluorescence intensities of the interest region across the red arrows along the red line of (a).

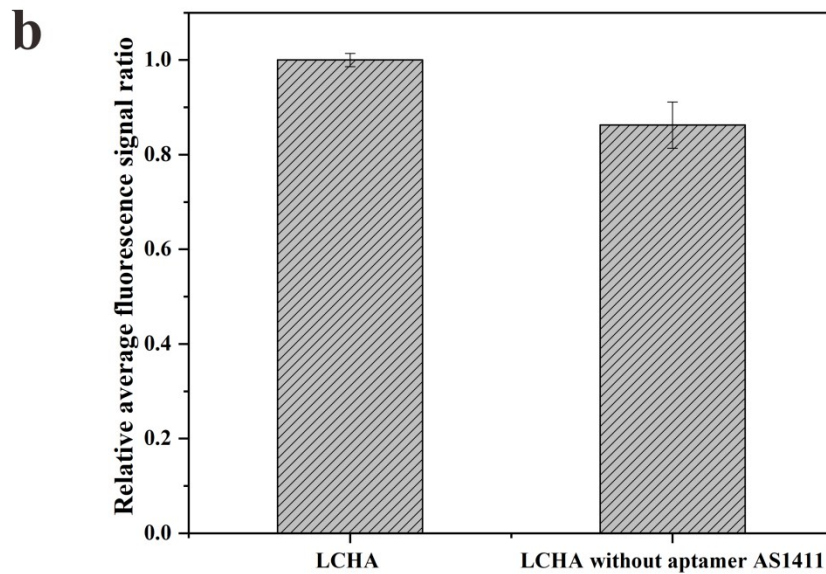
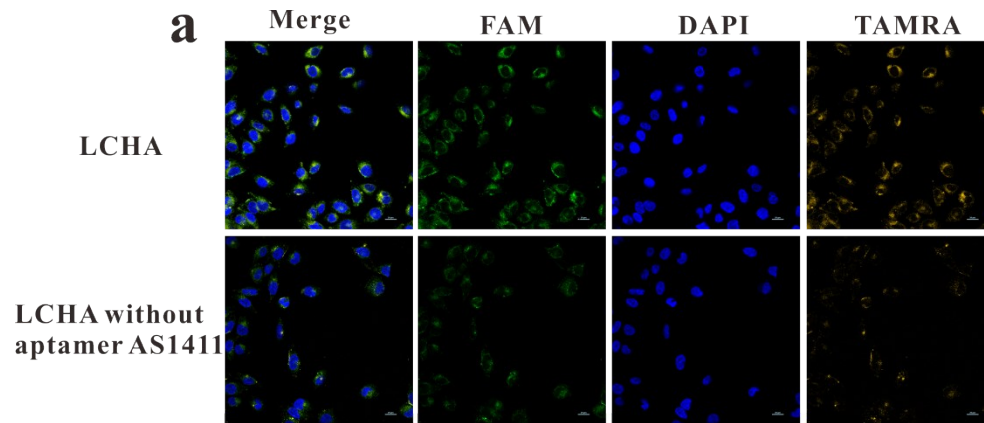


Fig. S6 Investigation performance of LCHA nanomachine and LCHA nanomachine without aptamer AS1411 for imaging miRNA-21 in living cancer cells. (a) confocal fluorescence images of MCF-7 cells treated with LCHA nanomachine or LCHA nanomachine without aptamer AS1411 for 37 °C at 4 h. The concentrations of the two nanomachines both were 50 nM, Scale bar = 20 μ m. (b) The values of relative average fluorescence signal ratio obtained from image (a) to represent the performance of LCHA nanomachine and LCHA nanomachine without aptamer AS1411 on cell imaging of the target miRNA-21. The relative average fluorescence signal ratio was calculated by normalized the average fluorescence signal ratio in MCF-7 cells incubated with LCHA nanomachine to 1.

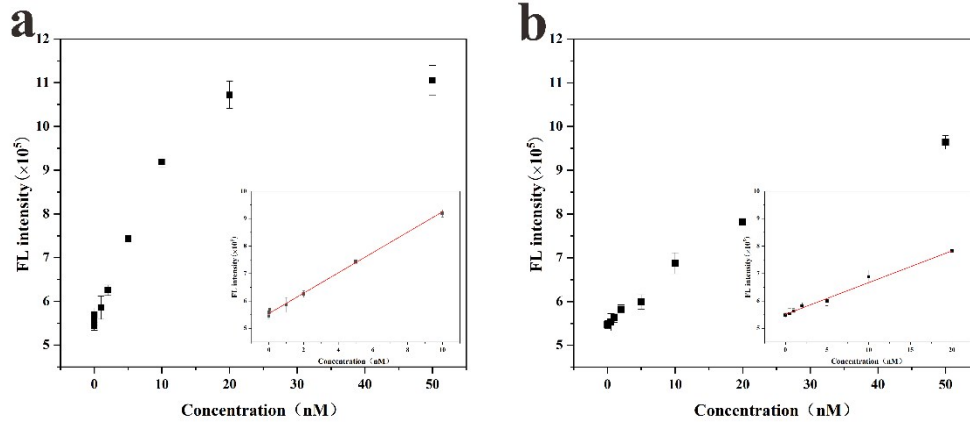


Fig. S7 The plots of FAM fluorescence intensity of LCHA nanomachine (a), free-CHA nanomachine (b) versus the different concentrations of target miRNA-21. Inset: the corresponding calibration curves of FAM fluorescence intensity against the concentration of target miRNA-21. The data error bars represented the standard deviation of three independent experiments.

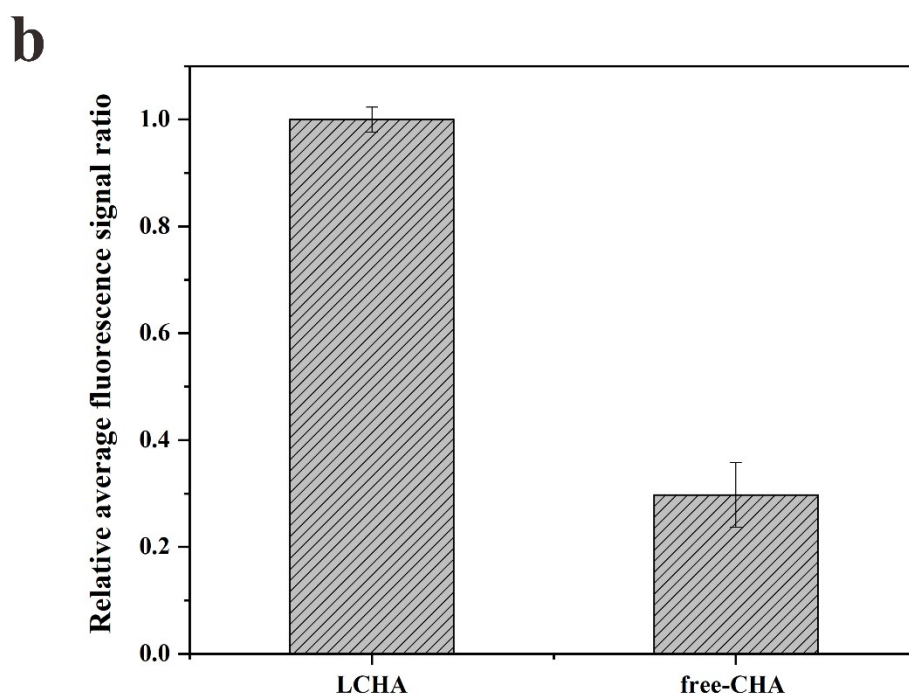
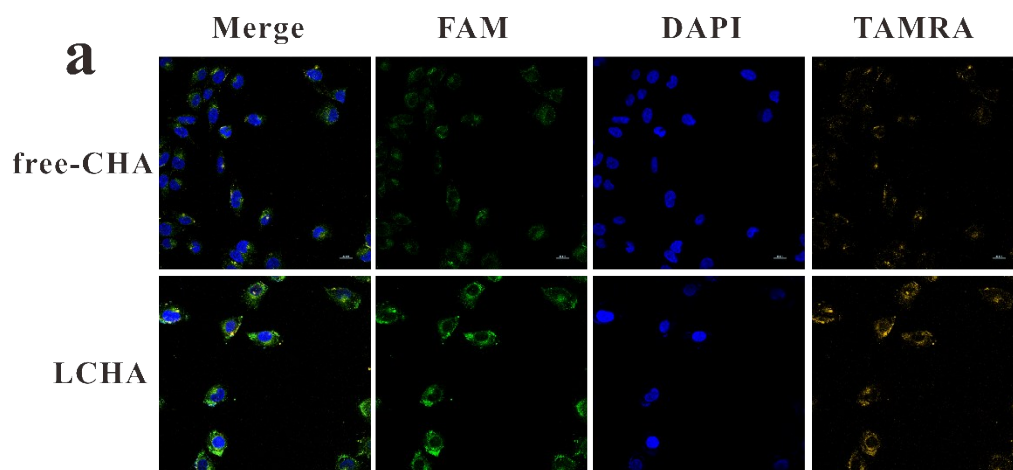


Fig. S8 Investigation performance of LCHA nanomachine and free-CHA nanomachine for imaging miRNA-21 in living cancer cells. (a) confocal fluorescence images of MCF-7 cells treated with LCHA nanomachine or free-CHA nanomachine for 37 °C at 4 h. The concentrations of the two nanomachines both were 50 nM. (b) The values of relative average fluorescence signal ratio obtained from image (a) to represent the performance of LCHA nanomachine and free-CHA nanomachine on cell imaging of the target miRNA-21. The relative average fluorescence signal ratio calculated by normalized that in MCF-7 cells incubated with LCHA nanomachine to 1, Scale bar = 20 μ m.

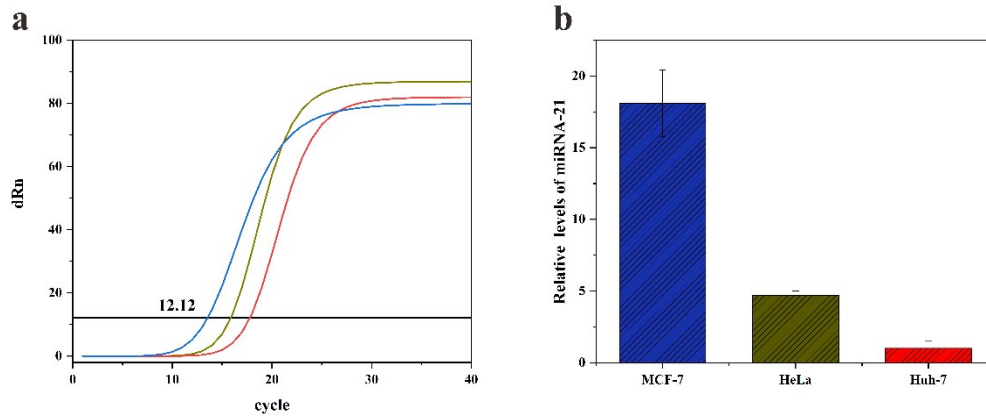


Fig. S9 Expression levels analysis of miRNA-21 in MCF-7 (blue), HeLa (deep yellow) and Huh-7 (red) cells. (a) Real-time fluorescence curves in qRT-PCR analysis. (b) Relative expression levels for miRNA-21.

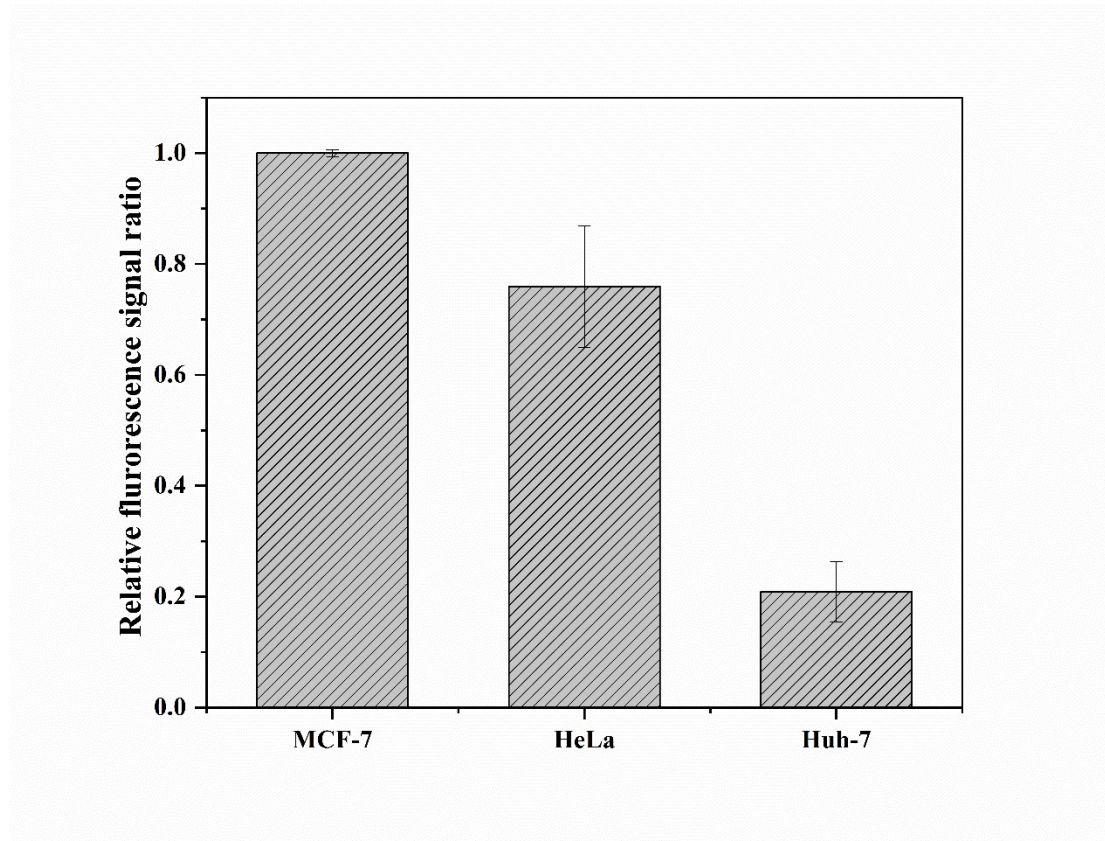


Fig. S10 Detection of miRNA-21 in different cell (MCF-7, HeLa and Huh-7) lysates. The relative fluorescence signal ratio calculated by normalized the fluorescence signal ratio in MCF-7 cells to 1 represent the relative expression level of miR-21 detected by our proposed assays.